PAN
ARCHIVES OF ACOUSTICS
Vol. **45**, No. 3, pp. 445–452 (2020)
DOI: 10.24425/aoa.2020.134060

Research Paper

Comparison of Acoustocerebrography Measurement and Magnetic Resonance Imaging Methods in the Assessment of White Matter Lesions in Patients with Atrial Fibrillation

Wioletta DOBKOWSKA-CHUDON[(1)], Mirosław WROBEL[(2)], Emilia FRANKOWSKA[(3)]
Arkadiusz ZEGADLO[(3)], Andrzej KRUPIENICZ[(4)], Andrzej NOWICKI[(5)], Robert OLSZEWSKI[(6)*]

[(1)] *District Hospital, Cardiology*
Radom, Poland

[(2)] *Fraunhofer Institute for Cell Therapy and Immunology IZI*
Leipzig, Germany

[(3)] *Department of Radiology, Military Institute of Medicine*
Warsaw, Poland

[(4)] *Medical University of Warsaw*
Warsaw, Poland

[(5)] *Department of Ultrasound, Institute of Fundamental Technological Research*
Polish Academy of Sciences
Warsaw, Poland

[(6)] *Department of Gerontology, Public Health and Didactics*
National Institute of Geriatrics, Rheumatology and Rehabilitation
Warsaw, Poland
[*] *Corresponding Author e-mail: robert.olszewski@spartanska.pl*

(*received March 10, 2020; accepted June 2, 2020*)

The brain is subject to damage, due to ageing, physiological processes and/or disease. Some of the damage is acute in nature, such as strokes; some is more subtle, like white matter lesions. White matter lesions or hyperintensities (WMH) can be one of the first signs of micro brain damage. We implemented the Acoustocerebrography (ACG) as an easy to use method designed to capture differing states of human brain tissue and the respective changes.

Aim: The purpose of the study is to compare the efficacy of ACG and Magnetic Resonance Imaging (MRI) to detect WMH in patients with clinically silent atrial fibrillation (AF).

Methods and results: The study included 97 patients (age 66.26 ± 6.54 years) with AF. CHA2DS2-VASc score (2.5 ± 1.3) and HAS BLED (1.65 ± 0.9). According to MRI data, the patients were assigned into four groups depending on the number of lesions: L0 – 0 to 4 lesions, L5 – 5 to 9 lesions, L10 – 10 to 29 lesions, and L30 – 30 or more lesions. Authors found that the ACG method clearly differentiates the groups L0 (with 0–4 lesions) and L30 (with more than 30 lesions) of WMH patients. Fisher's Exact Test shows that this correlation is highly significant ($p < 0.001$).

Conclusion: ACG is a new, easy and cost-effective method for detecting WMH in patients with atrial fibrillation. The ACG measurement methodology should become increasingly useful for the assessment of WMH.

Keywords: Acoustocerebrography; brain MRI; atrial fibrillation; white matter hyperintensities.

1. Introduction

The new ESC/ESH Guidelines (European Society of Cardiology and the European Society of Hypertension) for the management of arterial hypertension recommends the detection of subclinical organ damage related to hypertension as a very important clinical issue (Williams *et al.*, 2018). Hypertension

increases the spread of micro and macroscopic damage which is not always noticeable with clinical symptoms (Leary, Saver, 2003). With the development of modern imaging methods, such as magnetic resonance imaging (MRI) or computed tomography (CT), one can intravitally record these changes. Damage, that may not cause clinical symptoms includes silent strokes, microbleeds, white matter lesions or hyperintensities (WMH) (Selvetella *et al.*, 2003; Vermeer *et al.*, 2007; White *et al.*, 2018). Unfortunately, as earlier works from different clinical centers and researchers confirmed, the resulting changes in the brain have adverse effects on the clinical course of the patient, manifesting themselves in a wide spectrum of symptoms from cognitive disorders to depression or from dementia to cardiovascular diseases (Maillard *et al.*, 2012; Gorelick *et al.*, 2011; Hajjar *et al.*, 2011; Manie-ga *et al.*, 2016). WMH can be one of the first signs of micro brain damage. These changes can cause an entire spectrum of symptoms, from clinically silent to gait disturbances, cognitive dysfunctions, increases in the risk of stroke or ultimately death (Debette, Markus, 2010). Moreover, in patients with atrial fibrillation, white matter lesions are very common in the brain, early in the asymptomatic period (Mayasi *et al.*, 2018). Unfortunately, the current diagnostic methods of micro-injuries in the brain such as MRI, are expensive and not available to the wider population (Richoz, Fankhauser, 1997). CT scans, on the other hand, expose the patient to ionizing radiation and also have their limitations (Carpeggiani, Picano, 2016). Therefore, new non-invasive methods are sought that would allow the brain to be reviewed for asymptomatic damage. One such method is Acoustocerebrography (ACG). ACG is a non-invasive ultrasound-based method that allows non-invasive differentiation of tissue changes in the brain during the course of a disease's development (Dobkowska-Chudon *et al.*, 2018).

The purpose of the study is to compare the efficacy of ACG and MRI of the brain in the detection of WMH in patients with clinically silent atrial fibrillation.

2. Materials and methods

The study included 97 patients (57 male and 40 females, age 66.26 ± 6.54 years) who were surveyed in the clinical research with atrial fibrillation with documented persistent or paroxysmal AF. Patients with previous myocardial infarction, congestive heart failure, or a history of symptomatic cerebrovascular accident were excluded from the study.

This study was performed in accordance with the Declaration of Helsinki and approved by the Human Investigation Review Committee at the Military Institute of Medicine in Warsaw. Each participant provided written informed consent to participate in this study.

MRI was performed using a Siemens 1.5T scanner. Non-contrast sagittal 3D FLAIR images (1 mm slice thickness) were used to assess the number of WMH. We used semiautomatic software available on the GE Healthcare Advantage Workstation 4.6 (Volume Share 5). We counted every hyperintensities measuring at least 2 mm on each sagittal 3D FLAIR scan. Accordingly, lesions that were visible on two or more scans were counted several times. Patients were classified into diagnostic groups based on the total number of lesions or hyperintensities.

The ultrasonic data were collected using a method to record the transcranial time of flight (ToF). The signal was transmitted from the one side of the skull by an ultrasound probe and received by another ultrasound probe located at the opposite side of the skull. Based on the analysis of the human skull-brain-anatomy, it can be demonstrated that depending on the region, there are different conditions for the propagation of acoustic waves. The choice of the optimal position for transmitting/receiving transducers must take into account the acoustic wave attenuation (mostly in the skull bone areas) in a low MHz range. We utilized the acoustic frequency spectrum from 700 kHz up to 2.3 MHz. Regardless of the chosen location, the thickness of the skin, muscle and skull bones are considered to be constant – these structures are not changing with the systolic/diastolic heart phase and the final influence on the received signal in time can be disregarded. On the other hand, the contribution of the left and right Cerebrum, longitudinal cerebral fissure and cerebro-spinal fluid (CSF) to the received ultrasonic signal strongly depends on the cardiac cycle and the blood circulation in the brain tissue and are therefore the "Points of Interest" for the investigations. These parts of the brain have a substantial influence on the ToF due to the changes in the "global" density as well as the compression modulus K. The compression modulus K depends on the volume V, the volume change $\mathrm{d}V$ and the associated pressure change $\mathrm{d}p$. The density ρ is a ratio of the mass m and the volume V (Kinsler *et al.*, 2000):

$$c = \sqrt{\frac{K}{\rho}} = \sqrt{V \cdot \frac{\mathrm{d}p}{\mathrm{d}V \cdot \frac{m}{V}}} = V \cdot \sqrt{\frac{\mathrm{d}p}{\mathrm{d}V \cdot m}}.$$

Based on the above analysis, a simplified, layered structure of the cranial system can be adopted. Using this layered model of the human cranium as an input – together with the physical values of the different cranial tissues (Table 1), the propagation times of the acoustic signal as well as the signal attenuation along the flight path can be determined (Table 2) (Lynnerup *et al.*, 2005; Pakula *et al.*, 2009; Kremkau *et al.*, 1981; Fry, Barger, 1978). The values in the fields marked in gray in Table 2 remain constant during the heart cycles and can be ignored

Table 1. The basic parameters for the human skull-brain model.

Tissue	Density ρ [kg/m^3]	Sound speed c [m/s]	Acoustical impedance Z [kg/(m$^3\cdot$s)] $\cdot 10^6$	Attenuation at 1 MHz [dB/cm]
Cerebrum	1030	1515	1.56	2
Skull bones	1900	4080	7.75	10
CSF	1007	1498	1.51	0.003
Water	997	1483	1.478	0.003
Blood	1057	1580	1.67	0.2
Skin + fat	930	1480	1.38	1.5
Muscle	1002	1580	1.58	0.7

Table 2. Expected time of flights along the measurement path in brain layers (sample calculation).

	Skin	Muscle	Skull bones	CSF	Left cerebrum	Fissure	Right cerebrum	CSF	Skull bones	Muscle	Skin	Total:
Time [µs]	1.251	0.533	0.613	6.476	42.384	1.669	42.384	6.476	0.613	0.533	1.251	104.183

in further analysis. In our statistical analysis only differential and relative data is included, so the "static" skull elements do not affect the final results.

The acoustocerebrography method was described in our previous publication (Dobkowska-Chudon *et al.*, 2018). In short, ACG allows the capture of complex acoustical data dependent on the states and changes in human brain tissue. Basically, the signal transmitted through the skull is a compound pulse comprising of n discrete frequencies from f_1 to f_n, sampled with frequency $f_s \gg f_n$ (Kolany, Wrobel, 2016; Raboel *et al.*, 2012). The spectrum of the received signal is modified by the specific acoustical properties of the examined brain tissue, especially by the dispersion process occurring during the propagation of ultrasonic quasi-constant pulses in the tissue. Simultaneously, the phase angles of all n frequency components of the sounding pulse are measured in order to estimate the time of flight for each of n frequency components. The main idea of this method relies on the relation between the tissue density ρ, bulk modulus K and speed of sound c in the tissue under examination. The most important parameters estimated in the ACG method are attenuation coefficient and frequency-dependent attenuation, speed of sound and tissue elasticity. Speed of sound or, equivalently, the time of flight (ToF) of the respective pulses propagating along the brain path, can be inferred from phase relations between spectral components of the received spectra. The phase of received frequency components is measured with very high precision of 0.1° to 1° corresponding to about 5 ns precision in ToF measurements resulting in estimation of changes of speed of sound in the brain tissue equal to $\Delta c = 1.25$ m/s. The changes in local tissue density are also measured with high precision of $\Delta\rho/\rho = 1.6 \cdot 10^{-3}$. The bulk elasticity modulus K is calculated with a precision exceeding $\Delta K/K = 2.52 \cdot 10^{-5}$.

Figure 1 shows the typical "brain pulse" multispectral transmitted ultrasonic signal observed on the monitor during the examination. Depending on the location, size and nature of the vessels, and the shape and amplitude of the blood pressure, the shape of the signal varies. In the near-to-arterial region, the aortic valve closure results in incisor, which in the course of a period of the arterial blood pressure curve, is followed by arterial systolic pressure, incisor minimum, incisor maximum and arterial diastolic pressure. The sequence of edges minimum and maximum blurs towards the periphery and divides the pressure curve into a dicrotic notch (Kremkau *et al.*, 1981). Causes for this are hydrodynamic effects, which are caused by the nature of the vessel walls, as well as by the reflections of the pulse wave on the vessel forks.

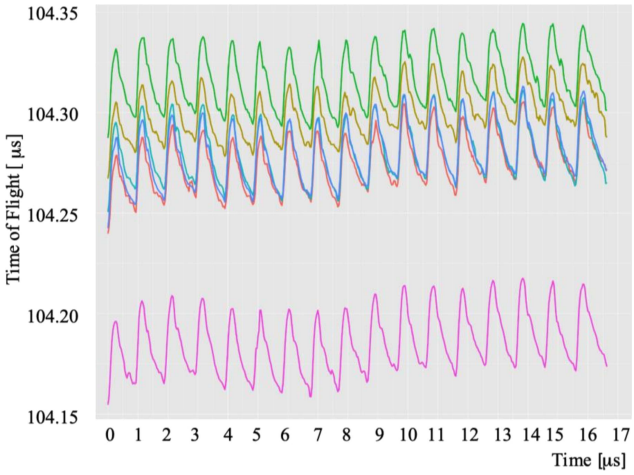

Fig. 1. Typical multispectral ultrasonic curves – here the 6 different frequencies, simultaneously recorded and plotted as the time of flight (ToF) curves. With the scanning system that was used, a maximum of 10 different frequencies can be sent and received at once. The signal sampling is 50 measurements per second (50 MPS).

Furthermore, in performing a basic validation of whether the ultrasonic signal is truly representative of the intracranial pressure, we ensure that there is in fact an oscillating pressure curve with the progressively decreasing notches present, indicating propagation of the cardiac pulse pressure signal. Further information is found in the pulse pressure signal, with the reversal of the first and second notches reflecting a state of disturbed autoregulation, for example.

The ACG examination time for each patient is equal to 180 seconds or approx. 150 heart beats. We performed the examination three times for each patient, and the average value was used for further processing using the multispectral ultrasound brain scanner UltraEASY2p^{TM} made by SonoMED Sp. z o.o., Poland in cooperation with Sonovum AG, Germany.

In this study, our focus was long-term brain tissue alteration due to WMH, so we had to filter the high dynamic data (as shown in Fig. 1) in such a way that the short time dynamic does not appear or interfere with our further analysis. We consolidated all of the raw data recorded during the examination sessions by eliminating amplification factors and using the fast Fourier transform. These acoustic spectral data were then used as the input data for the following statistical analysis (Schmude, 2017).

3. Statistical analysis

The groups of patients were compared using *Fisher's Exact Test* for categorical variables, and *Kruskal-Wallis-Test* for quantitative variables. The statistical significance was verified using p-values. The classification was done using a gradient-boosting machine and we used 10×5-fold cross-validation as the validation procedure. In the analysis of the dispersion phenomena related to the propagation of wide band ultrasound (700 kHz up to 2.3 MHz) in the brain tissue we have used eXtreme Gradient Boosting (XGBoost) tool, which is an algorithm widely used in applied machine learning and Kaggle competitions for structured or tabular data (Ding *et al.*, 2014). With XGBoost algorithm, target variables can be determined more precisely by combining several simpler and weaker models and making estimates. The XGBoost software addresses machine learning problems in the areas of regression, ranking and classification, being very efficient and providing reliable results. Supervised learning, as in our case, is a sub-area of machine learning and uses an existing database from which target variables can be derived. The training creates a model that predicts target variables applied to future data sets. Models are added until no further improvements in the predictions occur. Gradient boosting uses a special gradient algorithm, the so-called gradient descent algorithm, to add the models. The gradient boosting tree algorithm adds new branches that predict errors from previous branches and minimize errors or losses. The final forecasts are made by linking the trees or the branches. Statistical analyses were done using the R programming language for statistical computing and graphics (*https://www.r-project.org*) Version 3.3.0, with the packages gbm, plotROC and ggplot2.

4. Results

The characteristics of the 97 patients and their cardiovascular risk profiles are shown in Table 1. The vast majority (77.1%) were taking ACE inhibitors, 58.7% were taking betablocker, 51.5% were taking lipid-lowering therapies and 39.2% were on anticoagulants. The median age was 66.26 years and 42.1% of the participants were women. The CHA2DS2-VASc score was equal to 2.5 ± 1.3, and the mean HAS-BLED score was 1.65 ± 0.9. Medical history of the trial population is shown in the Table 3.

Table 3. Baseline characteristics.

	No	[%]
Coronary Artery Disease	49	50.5
Diabetes Mellitus	25	25.8
Smoking	12	12.4
Thyroid diseases	11	11.3
Vascular diseases	8	8.2
Asthma	4	4.1
Stroke in family	26	26.8
Heart diseases in family	20	20.6

According to the MRI data, the patients were divided into four groups based on the number of lesions: L0 – 0 to 4 hyperintensities, L5 – 5 to 9 hyperintensities, L10 – 10 to 29 hyperintensities, and L30 – 30 or more hyperintensities. As a result, it was demonstrated, that the ACG method could clearly differentiate the groups L0 (with 0–4 hyperintensities) and L30 (with more than 30 hyperintensities) of WML patients (Fig. 2). The groups of patients were compared using Fisher's Exact Test for categorical variables, and Kruskal-Wallis-Test for quantitative variables (Table 4). The statistical significance was verified using p-values.

Fisher test shows that best separated groups are pairs L0–L5 ($p = 0.0007$) and L10–L30 ($p = 0.0502$).

Continuous variables values in patient's groups were compared by Kruskal-Wallis test. Pairwise comparisons were tested using Dunn's pairwise comparisons test (p-value adjustment method: Bonferroni, p-value = 0.05).

The results for two most discriminative continuous variables are shown in Tables 5–8.

Acoustocerebrographic variables: AlphaQuo_75_3 and QuasiC_50_4: L0 with L5, L5 with L10, L10 with

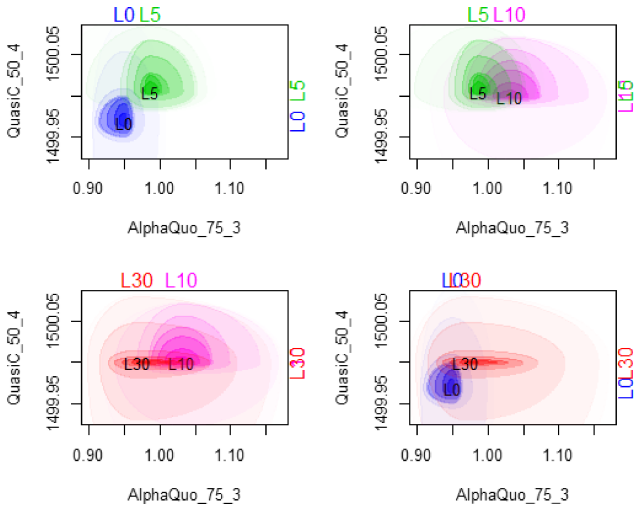

Fig. 2. Comparison of discriminative force of the two most discriminative.

Table 4. The results of Fisher Exact Test for pairs of patient's groups.

	Result of classification		
Original	L0	L5	
L0	9	5	$p = 0.0007$
L5	0	12	
	L10	L5	
L10	11	3	$p = 0.2117$
L5	6	6	
	L10	L30	
L10	12	2	$p = 0.0502$
L30	7	8	
	L0	L30	
L0	9	5	$p = 0.1431$
L30	5	10	

Original – original grouping of the sample

p – p-value of Fisher Exact Test

Table 5. Comparing values of variable QuasiC_50_4 in lesions groups. Kruskal-Wallis test chi-square statistics 8.48 with 3 degrees of freedom, $p = 0.0370$ (in the table are shown p-values of Dunn's test).

	L0	L10	L30
L10	0.16		
L30	0.46	1.00	
L5	0.04	1.00	1.00

L30, L0 with L30. The points L0, L30 represent the medians of the variables. The contours with different color intensity contain from most typical (the strongest intensity) up to less typical data (the weakest intensity). Each contour contains the same number of data.

Table 6. Grouping of lesions groups, using values of variable QuasiC_50_4 (mean rank – mean value of ranks in group, groups – grouping into groups a, b).

	Mean rank	Groups
L5	35.08	a
L10	31.39	ab
L30	28.53	ab
L0	17.96	b

Table 7. Comparing values of variable AlphaQuo_75_3 in lesions groups. Kruskal-Wallis test chi-square statistics 13.848 with 3 degrees of freedom, $p = 0.0031$ (in the table are shown p-values of Dunn's test).

	L0	L10	L30
L10	0.0013		
L30	0.2707	0.4799	
L5	0.1799	1.0000	1.0000

Table 8. Grouping of lesions groups, using values of variable AlphaQuo_75_3 (mean rank – mean value of ranks in group, groups – grouping into groups a, b).

	Mean rank	Groups
L10	38.42	a
L5	29.75	ab
L30	28.00	ab
L0	16.07	b

5. Discussion

The first conclusion of our study was that Acoustocerebrography is a method that can provide quantitative information about the number of WMH confirmed by MRI. This may mean that for the first time we have found a non-invasive tool for diagnosing WMH in the brain in patients with both atrial fibrillation and hypertension. It is a very important finding because WMH is a pathology that often occurs in the human brain in 11% to 21% of adults and increases with age reaching the rate of over 90% in patients over 80 years of age (Freedman *et al.*, 2016; Bokura *et al.*, 2006). White matter lesions or hyperintensities are observed in the brain (mostly by MRI) of older people, which are associated with increased risks of developing depression, having strokes, and suffering from dementia (Van Dijk *et al.*, 2008). Therefore, it is extremely valuable to find a cost-effective tool that will quickly and non-invasively allow the screening of the brain in broad populations of adults. ACG is such a method; as we have shown in the previous study, it allows for the differentiation of the signal that indicates pathological processes in the brain in hypertensive patients. In a previous study published by our group, we showed

that we were able to find differences in the ultrasound signal of the brain measured by ACG between patients with and without hypertension in the group with atrial fibrillation (Dobkowska-Chudon *el al.*, 2018). This observation is particularly important from a clinical point of view because it gives us quantitative information about the function of the brain which is particularly vulnerable to destruction by both physiological factors such as aging as well as pathological ones such as hypertension or atrial fibrillation.

The second discovery of our study was that ACG is a method that can provide information about the number of WMH. It is especially important that ACG differentiates the number of WMH, and in particular the number of WMH exceeding 30, to an almost healthy brain with a WMH number less than 5. Yamauchi *et al.* (2002) have proved that change in the number of WMH is a predictive factor of the state leading to ischemic strokes. The authors show that severe WMH was an independent predictor of a subsequent stroke, even after controlling for the risk factor status during follow up. It was a very important study that indicates that there is a need to track the increasing number of WMH in the brains of patients in order to protect them from suffering strokes. According to an epidemiological study, the worldwide prevalence of AF is 596.2 and 373.1 per 100,000 men and women, respectively (Chugh *et al.*, 2014). The group of patients with atrial fibrillation selected in this study and our previous studies show that ACG may allow for a screening of the brain for patients with hypertension (Dobkowska-Chudon *et al.*, 2018). Reinhard *et al.* (2012) showed that the numbers of WMH correlated with NT-ProBNP in patients with diabetes and Wei *et al.* (2018) confirmed correlation of WMH with rheumatic disease. Moreover, this new data shows that WMH is a kind of biological marker for a wide spectrum of different diseases, so ACG potentially could be used as a brain screening tool for various other disease states. Acoustocerebrography is a non-invasive, nontime consuming and an easy-to-use procedure. Analysing the results of our current and earlier research, as well as the reports from the literature, we can conclude that ACG is a useful method for cardiologists. It allows one to assess the risk of stroke as well as to estimate the impairment of dementia and cognitive functions. Of course, this thesis requires further clinical trials on a larger population of patients.

At this stage of study we should underline the limitation of our findings in that: (i) we examined a medium-sized group of patients in only one health center; (ii) we provided an offline, manual calculation of the number of WMH; and (iii) we used a 1.5 T MRI scanner with lower accuracy in assessing WMH, compared to currently available ones (e.g. the high-field strength 3.0 T and ultra-high resolution 7.0 T MRI) which have shown additional diagnostic benefits in the recognition of this cerebral pathology (De Cocker *et al.*, 2018). Further, the authors did not take into account possible micro-bleeds which might also potentially affect the ACG results. Regardless of these limitations, the results were very promising and further clinical information is important and a subsequent study should examine on a larger group of patients.

6. Conclusions

ACG is a new, effective non-invasive method for detecting WMH in patients with atrial fibrillation. The ACG measurement methodology may become increasingly useful for quantitative assessment of WMH.

Acknowledgements

This work was supported by the Development Bank of Saxony – EFRE Grant No.100109012/990.301573.

Declaration of interests

The authors have read the journal's policy and have the following conflicts:

Mirosław Wrobel serves as the CTO of Sonovum AG – Leipzig, Germany, and holds potential financial interest through patented technology. To fulfill the study's objectives an "UltraEASY2p^{TM} ACG System" was built in cooperation with SonoMED Sp. z o.o. – Warsaw, Poland for data acquisition. Sonovum and SonoMED provided service and maintenance of the systems during the study.

Wioletta Dobkowska-Chudon, Emilia Frankowska, Arkadiusz Zegadlo, Andrzej Krupienicz, Andrzej Nowicki, Robert Olszewski – Declaration of interest: None.

References

1. Bokura H. *et al.* (2006), Silent brain infarction and subcortical white matter lesions increase the risk of stroke and mortality: a prospective cohort study, *Journal of Stroke and Cerebrovascular Diseases*, **15**(2): 57–63, doi: 10.1016/j.jstrokecerebrovasdis.2005.11.001 .

2. Carpeggiani C., Picano E. (2016), The radiology informed consent form: recommendations from the European Society of Cardiology position paper, *Journal of Radiological Protection*, **36**(2): S175–S186, doi: 10.1088/0952-4746/36/2/s175.

3. Chugh S.S. *et al.* (2014), Worldwide epidemiology of atrial fibrillation – A Global Burden of Disease 2010 Study, *Circulation*, **129**(8): 837–847, doi: 10.1161/circulationaha.113.005119.

4. De Cocker L.J. *et al.* (2018), Clinical vascular imaging in the brain at 7T, *NeuroImage*, **168**: 452–458, doi: 10.1016/j.neuroimage.2016.11.044.

5. Debette S., Markus H.S. (2010), The clinical importance of white matter hyperintensities on brain mag-

netic resonance imaging: systematic review and meta-analysis, *BMJ*, **341**: c3666, doi: 10.1136/bmj.c3666.

6. Ding S., Xu X., Nie R. (2014), Extreme learning machine and its applications, *Neural Computing and Applications*, **25**(3–4): 549–556, doi: 10.1007/s00521-013-1522-8.

7. Dobkowska-Chudon W. *et al.* (2018), Detecting cerebrovascular changes in the brain caused by hypertension in atrial fibrillation group using acoustocerebrography, *PLoS ONE*, **13**(7): e0199999, doi: 10.1371/journal.pone.0199999.

8. Freedman B., Potpara T.S., Lip G.Y. (2016), Stroke prevention in atrial fibrillation, *Lancet*, **388**(10046): 806–817, doi: 10.1016/S0140-6736(16)31257-0.

9. Fry F., Barger J. (1978), Acoustical properties of the human skull, *Journal of the Acoustical Society of America*, **63**(5): 1576–1590, doi: 10.1121/1.381852.

10. Gorelick P.B. *et al.* (2011), Vascular contributions to cognitive impairment and dementia, *Stroke*, **42**(9): 2672–2713, doi: 10.1161/str.0b013e3182299496.

11. Hajjar I. *et al.* (2011), Hypertension, white matter hyperintensities, and concurrent impairments in mobility, cognition, and mood: The Cardiovascular Health Study, *Circulation*, **123**(8): 858–865, doi: 10.1161/circulationaha.110.978114.

12. Kinsler L.E., Frey A., Coppens A.B., Sanders J.V. (2000), *Fundamentals of Acoustics*, John Wiley and Sons, New York.

13. Kolany A., Wrobel M. (2016), Some algebraic and algorithmic problems in acoustocerebrography, *Bulletin of the Section of Logic*, **45**(3/4): 239–256, doi: 10.18778/0138-0680.45.3.4.07.

14. Kremkau F.W., Barnes R.W., McGraw P.C. (1981), Ultrasonic attenuation and propagation speed in normal human brain, *Journal of the Acoustical Society of America*, **70**(1): 29–38, doi: 10.1121/1.386578.

15. Leary M.C., Saver J.L. (2003), Annual incidence of first silent stroke in the United States: a preliminary estimate, *Cerebrovascular Diseases*, **16**(3): 280–285, doi: 10.1159/000071128.

16. Lynnerup N., Astrup J., Sejrsen B. (2005), Thickness of the human cranial diploe in relation to age, sex and general body build, Head & Face Medicine, **1**(1): 13, doi: 10.1186/1746-160X-1-13.

17. Maillard P. *et al.* (2012), Effects of systolic blood pressure on white-matter integrity in young adults in the Framingham Heart Study: a cross-sectional study, *Lancet Neurology*, **11**(12): 1039–1047, doi: 10.1016/S1474-4422(12)70241-7.

18. Maniega S.M. *et al.* (2016), Integrity of normal-appearing white matter: influence of age, visible lesion burden and hypertension in patients with small-vessel disease, *Journal of Cerebral Blood Flow & Metabolism*, **37**(2): 644–656, doi: 10.1177/0271678X16635657.

19. Mayasi Y. *et al.* (2018), Atrial fibrillation is associated with anterior predominant white matter lesions in patients presenting with embolic stroke, *Journal of Neurology, Neurosurgery & Psychiatry*, **89**(1): 6–13, doi: 10.1136/jnnp-2016-315457.

20. Pakula M., Padilla F., Laugier P. (2009), Influence of the filling fluid on frequency – dependent velocity velocity and attenuation in cancellous bones between 0.5 and 2.5 MHz, *Journal of the Acoustical Society of America*, **126**(6): 3301–3310, doi: 10.1121/1.3257233.

21. Raboel P.H., Bartek J., Andresen M., Bellander B.M., Romner B. (2012), Intracranial pressure monitoring: invasive versus non-invasive methods – a review, *Critical Care Research and Practice*, **2012**: 950393, doi: 10.1155/2012/950393.

22. Reinhard H. *et al.* (2012), Plasma NT-proBNP and white matter hyperintensities in type 2 diabetic patients, *Cardiovascular Diabetology*, **11**(1): 119, doi: 10.1186/1475-2840-11-119.

23. Richoz B., Fankhauser H. (1997), Cerebral magnetic resonance imaging: indications and contraindications [in French], *Revue Médicale Suisse Romande*, **117**(12): 931–945.

24. Schmude P. (2017), Feature selection in multiple linear regression problems with fewer samples than features, [in:] Rojas I., Ortuño F. (Eds), *Bioinformatics and Biomedical Engineering. IWBBIO 2017. Lecture Notes in Computer Science*, Vol. 10208, pp. 85–95, Springer, Cham.

25. Selvetella G. *et al.* (2003), Left ventricular hypertrophy is associated with asymptomatic cerebral damage in hypertensive patients, *Stroke*, **34**(7): 1766–1770, doi: 10.1161/01.str.0000078310.98444.1D.

26. Van Dijk E.J., Prins N.D., Vrooman H.A.., Hofman A, Koudstaal P.J., Breteler M. (2008), Progression of cerebral small vessel disease in relation to risk factors and cognitive consequences – Rotterdam Scan study, *Stroke*, **39**(10): 2712–2719, doi: 10.1161/strokeaha.107.513176.

27. Vermeer S.E., Longstreth W.T., Jr, Koudstaal P.J. (2007), Silent brain infarcts: a systematic review, *Lancet Neurology*, **6**(7): 611–619, doi: 10.1016/S1474-4422(07)70170-9.

28. Wei C., Zhang S., Liu J., Yuan R., Liu M. (2018), Relationship of cardiac biomarkers with white matter hyperintensities in cardioembolic stroke due to atrial fibrillation and/or rheumatic heart disease, Medicine (Baltimore), **97**(33): e11892, doi: 10.1097/MD.0000000000011892.

29. White W.B. *et al.* (2018), Relationships among clinic, home, and ambulatory blood pressures with small vessel disease of the brain and unctional status in older people with hypertension, *American Heart Journal*, **205**: 21–30, doi: 10.1016/j.ahj.2018.08.002.

30. Williams B. *et al.* (2018), ESC Scientific Document Group. 2018 ESC/ESH Guidelines for the management of arterial hypertension, *European Heart Journal*, **39**(33): 3021–3104, doi: 10.1093/eurheartj/ehy339.

31. Wrobel M., Dabrowski A., Kolany A., Olak-Popko A., Olszewski R., Karlowicz P. (2015), On ultrasound classification of stroke risk factors from randomly chosen respondents using non-invasive multi-spectral ultrasonic brain measurements and adaptive profiles, *Biocybernetics and Biomedical Engineering*, **36**(1): 18–28, doi: 10.1016/j.bbe.2015.10.004.

32. Yamauchi H., Fukuda H., Oyanagi C. (2002), Significance of white matter high intensity lesions as a predictor of stroke from arteriolosclerosis, *Journal of Neurology, Neurosurgery & Psychiatry*, 72(5): 576–582, doi: 10.1136/jnnp.72.5.576.